

Universality and the three-body parameter of helium-4 trimers

Pascal Naidon¹, Emiko Hiyama¹, and Masahito Ueda²
¹*RIKEN Nishina Centre, RIKEN, Wako 351-0198, Japan, and*
²*Department of Physics, University of Tokyo,*
7-3-1 Hongo, Bunkyo-ku, Tokyo 113-0033, Japan
(Dated: November 6, 2018)

We consider a system of three helium-4 atoms, which is so far the simplest realistic three-body system exhibiting the Efimov effect, in order to analyse deviations from the universal Efimov three-body spectrum. We first calculate the bound states using a realistic two-body potential, and then analyse how they can be reproduced by simple effective models beyond Efimov's universal theory. We find that the non-universal variations of the first two states can be well reproduced by models parametrized with only three quantities: the scattering length and effective range of the original potential, and the strength of a small three-body force. Furthermore, the three-body parameter which fixes the origin of the infinite set of three-body levels is found to be consistent with recent experimental observations in other atomic species.

I. INTRODUCTION

The universal attraction found by V. Efimov [1] for any quantum system of three particles interacting through short-range interactions with a large scattering length has now been evidenced in many experiments using ultra-cold atoms [2–17]. In particular, Efimov trimers, i.e. three-body bound states resulting from this attraction, were observed as a function of the scattering length. Because these trimers are unnaturally large compared with the range of the interactions, they have universal properties determined solely by the universal attraction and a few parameters. In particular, their spectrum has a simple structure with discrete scale invariance. This was confirmed experimentally to some degree, but there appeared quantitative deviations from this structure.

One of the main reasons is the fact that at most the first two states of the spectrum could be observed so far. It is known that these first states do not follow accurately the universal behaviour expected for the higher excited states (more loosely bound states), because their size is not very large compared to the range of the interactions and therefore they still depend on the details of these interactions. However, it is quite involved to correctly describe these interactions for three atoms because of their complex hyperfine structure and the lack of knowledge of the three-body potential surfaces. For this reason, experimental results have been interpreted so far using either interaction-dependent corrections to the universal theory of Efimov [15, 16, 18, 19], or by other effective models reproducing the two-body physics in the energy range of the observed trimers [20–22].

While these effective approaches could reproduce the experimental results to some extent, it remains unclear on a theoretical basis why they could do so. For example, corrections to the Efimov universal theory sometimes required to introduce an ad-hoc variation of a 3-body parameter to explain the data [15, 16, 22]. Another puzzling fact is that effective two-body model approaches could reproduce some of the deviations from universal theory observed in the experimental data, suggesting that they could be explained by two-body interactions only [20–22]. While it is established

that in general the knowledge of two-body interactions only is not enough to accurately determine the energy of Efimov trimers [23], the contribution from realistic two-body interactions to the short-range 3-body phase and non-universal deviations are not fully understood.

The purpose of this paper is to clarify these issues by testing the effective approaches with respect to the numerically exact solution of a realistic theoretical model. We choose ${}^4\text{He}_3$, as it is the simplest triatomic system with van der Waals interactions which exhibits the Efimov attraction [24–28].

The paper is organised as follows. In section II, we review some of the effective models used to describe Efimov trimer experiments. In section III, we present realistic calculations for ${}^4\text{He}_3$, and how they are reproduced by these effective models.

II. EFFECTIVE MODELS FOR EFIMOV PHYSICS

A. Efimov's universal theory

The essence of the Efimov effect is the appearance of an effective attractive potential $-s_0^2/R^2$ attraction between three particles with very large scattering length. Here, s_0 is a number approximately equal to 1.00624 for identical bosonic particles, and R denotes the hyper-radius (average distance between particles),

$$R^2 = \frac{1}{3}(r_{12}^2 + r_{23}^2 + r_{31}^2), \quad (1)$$

where r_{12}, r_{23} , and r_{31} are the three particles' relative distances. This attraction can lead to the existence of three-body bound states, the so-called Efimov trimers. Because it is a long-range attraction, trimers with sufficiently small binding energy extend to large distances where the interactions are negligible. The only effect of interactions is to set short-distance boundary conditions on the three-body wave function. The first boundary condition occurs when two particles come close to one another, but within a distance r larger than the range of their interaction. There, the wave

function ψ has to satisfy the Bethe-Peierls boundary condition

$$\psi \underset{r_{ij} \rightarrow 0}{\propto} \frac{1}{r_{ij}} - \frac{1}{a}, \quad (2)$$

where a is the s-wave scattering length of the two-body interaction, which fixes the phase of the two-body wave function accumulated from short distance at low energy. The second boundary condition occurs when three particles come close together, but still at distances R larger than the range of their interactions. The wave function has to satisfy the Efimov boundary condition

$$\psi \underset{R \rightarrow 0}{\propto} \frac{1}{R} \sin(s_0 \log(\Lambda R)), \quad (3)$$

where Λ is the so-called Efimov three-body parameter, which fixes the accumulated phase of the three-body wave function at low energy.

The Efimov theory thus relies on only two parameters, a and Λ , to fully describe the three-body physics in the low-energy and large a regime. When normalised in units of Λ , the trimer energy spectrum exhibits a universal structure as a function of $a\Lambda$, represented in Fig. 5. There is an accumulation point in the spectrum at $a = \infty$, that is when the two-body interaction is resonant, and the whole spectrum is invariant by a discrete scale transformation, namely multiplying all distances by $e^{\pi/s_0} \approx 22.7$, which follows from Eq. (3). The wave functions and energies can be calculated numerically by either solving the 3-body free Schrödinger equation with conditions (2) and (3), or equivalently solving its corresponding integral equation which is known as the Skorniakov- Ter-Martirosian equation [29],

$$\left(\frac{1}{a} - \sqrt{\frac{3}{4}p^2 - \varepsilon} \right) F(p) + \frac{2}{\pi} \int_0^P dq \ln \frac{p^2 + q^2 + pq - \varepsilon}{p^2 + q^2 - pq - \varepsilon} F(q) = 0 \quad (4)$$

where F is the unknown function (related to the full wave function Ψ), and $\varepsilon = \frac{mE}{\hbar^2}$ is the renormalised energy E . Here, the upper bound P of the integral sets the three-body phase, and can be related to the Efimov three-body parameter by [22]:

$$P = \Lambda \exp\left(-\frac{\arctan s_0 + \pi n}{s_0}\right)$$

B. Non-universal models

1. Non-universal corrections

The deviations of two-body physics from universality at low energy are well known and can be encoded in the energy variation of the two-body phase shift $\delta(E)$, or equivalently a two-body scattering length $a(E)$. At low energy, we have the following effective-range low-energy expansion:

$$\frac{1}{a(E)} \equiv -k \cot \delta(E) = \frac{1}{a} - \frac{1}{2} r_e k^2 + \dots \quad (5)$$

where $k = \sqrt{mE}/\hbar$. The universal limit corresponds to the first term, which is set by the zero-energy scattering length a . The next order defines the effective range r_e . It is straightforward to generalise Eq. (4) to the non-universal regime by replacing the zero-energy scattering length a by the energy-dependent scattering length $a(E)$ [22, 30]. Likewise, the cutoff P is expected to be replaced by an energy-dependant quantity $P(E)$ [22]. With these replacements, Eq. (4) corresponds to the most general contact model with energy-dependent boundary conditions.

Although the energy dependence of $a(E)$ is generally known, that of $P(E)$ is presently unknown. It is one of the purposes of this paper to investigate this dependence from comparison with other models.

2. Two-body effective interaction

Another approach is to replace the real interaction by a simple effective interaction with the same low-energy spectrum. One possible choice is a Gaussian potential [31, 32]:

$$V(r) = -V_0 e^{-(r/r_0)^2}, \quad (6)$$

which is parametrised by V_0 and r_0 to reproduce both the scattering length and effective range. Another convenient choice is a separable interaction [20–22]:

$$\hat{V} = V_0 |\phi\rangle \langle \phi| \quad (7)$$

where the state $|\phi\rangle$ can also be chosen to be a Gaussian function $\phi(r) = e^{-(r/r_0)^2}$ for simplicity. The advantage of separable potentials is that they have formal similarities with contact interactions, and lead to a simple integral equation similar to Eq. (4):

$$\left(\frac{1}{a(E)} - \sqrt{\frac{3}{4}p^2 - \varepsilon} \right) F(p) + \frac{2}{\pi} \int_0^\infty dq \ln \frac{G(r_0^2(p^2 + q^2 + pq - \varepsilon))}{G(r_0^2(p^2 + q^2 - pq - \varepsilon))} e^{\frac{3}{8}r_0^2(q^2 - p^2)} F(q) = 0 \quad (8)$$

where $G(x) = \exp[\int_x^\infty \frac{e^{-t}}{t} dt]$. One can check that the integrand of (8) tends to that of (4) at low momenta, but decays at high momenta $q \gtrsim 1/r_0$, which removes the need to introduce an upper bound to the integral.

III. REALISTIC AND EFFECTIVE CALCULATIONS FOR ${}^4\text{He}_3$

A. Realistic calculations with LM2M2 potentials

To model ${}^4\text{He}$ interactions realistically, we choose the LM2M2 potential [33] to describe the two-body interactions. This potential has a repulsive hard core at short distance, and a van der Waals tail $-C_6/r^6$ at large distance, as shown in Fig. 1. Its scattering length is 100.01 Å which is 18.6 times the van

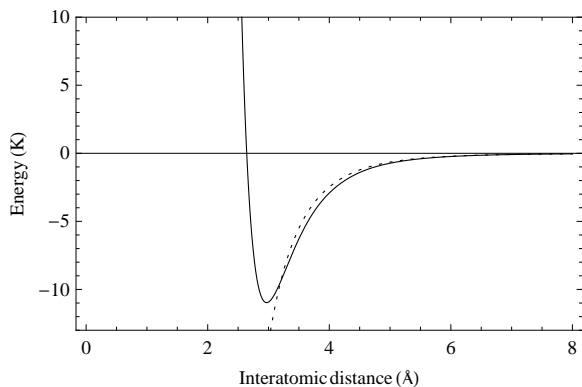


Figure 1: LM2M2 potential [33] used for the realistic calculations. The dotted curve indicates the van der Waals asymptote $-C_6/r^6$.

der Waals length $l_{\text{vdW}} = (mC_6/\hbar)^{1/4}$. The three-body interaction has been shown to bring only small corrections [34–36], and we neglect it in this study. Thus, in our calculation, the 3-body phase which fixes the energy of Efimov trimers builds up only from the LM2M2 two-body interaction.

The 3-body Schrödinger equation with the LM2M2 potential is solved numerically using the Gaussian expansion method (GEM). This method was proposed as a means to perform accurate calculation for three- and four-body systems [37]. In this method, a well-chosen set of Gaussian basis function is used, forming an approximately complete set in a finite coordinate space, so that one can describe accurately both short-range correlation and the long-range asymptotic behaviour of the wavefunction for bound systems as well as for scattering states. It was demonstrated that the GEM provides the same caliber of numerical precision as, for example, the Faddeev-Yakubovsky method for ^3H (^3He) and ^4He , and can be used to address various kinds of few-body problems in atomic, baryonic and quark-level systems [37].

In order to solve three-body ^4He trimer problem, we use three sets of Jacobi coordinates illustrated in Fig. 2.

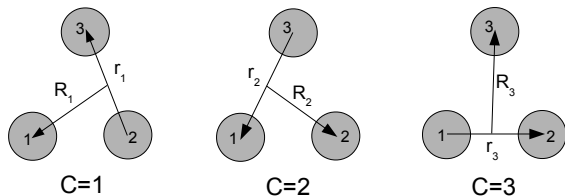


Figure 2: Jacobi coordinates for all the rearrangement channels ($c = 1 \sim 3$) of ^4He trimer system. Three ^4He atoms are to be symmetrized.

The Schrödinger equation and the total Hamiltonian are given by

$$(H - E) \Psi_{JM} = 0, \quad (9)$$

$$H = T + V(r_1) + V(r_2) + V(r_3), \quad (10)$$

where T is the kinetic-energy operator and $V(r_1)$, $V(r_2)$ and $V(r_3)$ are the interactions between two ^4He atoms, described by the LM2M2 potential $V(r)$.

The total three-body wavefunction is described as a sum of amplitudes for all rearrangement channels ($c = 1 \sim 3$) of Fig. 2:

$$\Psi_{JM} = \sum_{c=1}^3 \sum_{n,N} \sum_{\ell,L} C_{nlNL}^{(c)} [\phi_{nl}^{(c)}(\mathbf{r}_c) \psi_{NL}^{(c)}(\mathbf{R}_c)]_{JM}. \quad (11)$$

We take the functional forms of $\phi_{nlm}(\mathbf{r})$, $\psi_{NLM}(\mathbf{R})$ as

$$\begin{aligned} \phi_{nlm}(\mathbf{r}) &= r^l e^{-(r/r_n)^2} Y_{lm}(\hat{\mathbf{r}}), \\ \psi_{NLM}(\mathbf{R}) &= R^L e^{-(R/R_N)^2} Y_{LM}(\hat{\mathbf{R}}), \end{aligned} \quad (12)$$

where the Gaussian range parameters are chosen according to geometrical progressions:

$$\begin{aligned} r_n &= r_1 a^{n-1} \quad (n = 1, \dots, n_{\text{max}}), \\ R_N &= R_1 A^{N-1} \quad (N = 1, \dots, N_{\text{max}}). \end{aligned} \quad (13)$$

The eigenenergies E in Eq.9 and the coefficients C in Eq.11 are determined by the Rayleigh-Ritz variational method.

Although the scattering length of ^4He is already large compared to the range of its two-body potential $V(r)$, we did several calculations for rescaled potentials $\lambda V(r)$ in order to cause a divergence of the scattering length, as was done in previous studies [24, 25, 27]. This enables us to mimic the broad Feshbach resonances used in ultra-cold atom experiments [38], and better appreciate the Efimov structure of the spectrum. The scattering length a diverges for $\lambda = 0.97412$, while the physical results for real ^4He correspond to $\lambda = 1$. As λ is varied near the divergence of a , the effective range r_e also changes but always remains positive and on the order of the scaled van der Waals length $\lambda^{1/4} l_{\text{vdW}}$, and the ratio r_e/a remains a monotonic function of λ , as shown in Fig. 3. For this reason, we choose to report our results as a function of the scattering length in units of the effective range, rather than λ itself.

The LM2M2 potential supports one two-body bound state and its energy variation with the scattering length is represented in Fig. 4. When the scattering length becomes smaller than its physical value ($\lambda \gtrsim 1.0$), this dimer energy significantly deviates from the universal limit of small binding energy and large scattering length (Eq. (14) with $a(E) \rightarrow a$). The results for three atoms are shown in Fig. 5. Our results are in very good agreement with the most accurate calculations using the LM2M2 potential [39, 40]. One can see that the first two trimers' energies qualitatively follow Efimov's universal spectrum, but as in the two-body case, there are significant deviations for small scattering lengths and deep energies.

B. Calculation with non-universal corrections

We first attempt to reproduce the previous results by including non-universal corrections to the Efimov

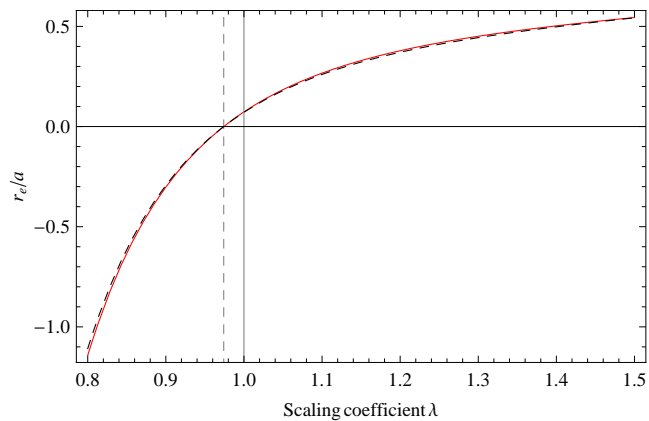


Figure 3: Ratio between the effective range r_e and scattering length a of the scaled LM2M2 potential, as a function of the scaling coefficient λ . The vertical solid line indicates the physical value ($\lambda = 1$). The dashed vertical line indicates the scaling where the scattering length diverges ($1/a \rightarrow 0$). The dashed curve shows the result based on the analytical formula (16) using the values of \bar{a} and a as a function of λ .

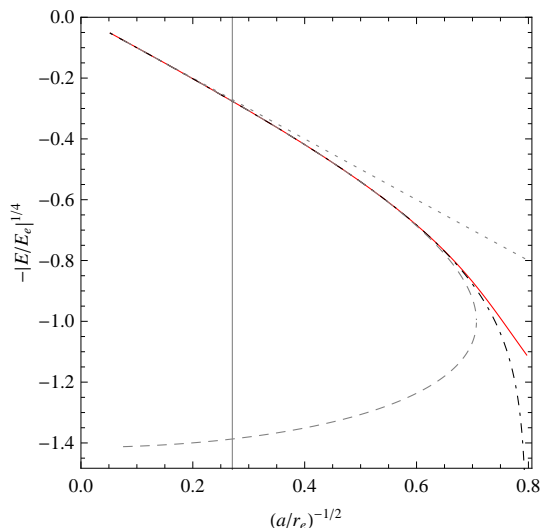


Figure 4: Helium 4 dimer energy E as a function of scattering length a . To clarify the figure, these quantities are normalised to $E_e = \hbar^2/mr_e^2$ and r_e , and raised to the power $1/4$ and $-1/2$, respectively. The solid red curve corresponds to the dimer of the LM2M2 potential scaled by a coefficient λ . The physical scattering length of helium 4 ($\lambda = 1$) is indicated by the vertical gray line. The dotted line represents the universal limit of small binding energy and large scattering length [Eq. (14) with $a(E) \rightarrow a$]. The dashed curve represents the two solutions of the effective range approximation of Eq. (14). The dotted-dashed curve corresponds to the results of the separable Gaussian potential (7).

theory. For each value of λ , we can determine the energy dependence $a(E)$ of the scattering length of the scaled LM2M2 potential $\lambda V(r)$. The energy E_{2B} of the two-body bound state is then readily obtained from the equation:

$$E_{2B} = -\frac{\hbar^2}{m[a(E_{2B})]^2} \quad (14)$$

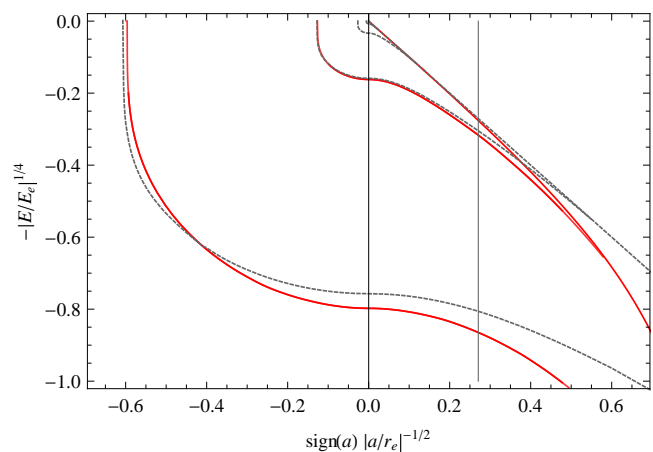


Figure 5: Efimov spectrum for helium 4: trimer energy E as a function of the scattering length a . To clarify the figure, these quantities are normalised to $E_e = \hbar^2/mr_e^2$ and r_e , and raised to the power $1/4$ and $-1/2$, respectively. The zero of the energy axis corresponds to the three-body threshold. The red solid curves are the energy curves obtained by scaling the LM2M2 potential. Both trimers and dimer (rightmost curve) are displayed. The vertical gray line indicates the scattering length corresponding to the unscaled potential, *i.e.* physical helium 4. The dashed curves correspond to the Efimov trimer spectrum according to the universal theory. The 3-body parameter is adjusted to match the first excited trimer state. The straight dashed line corresponds to the dimer energy in the universal limit of large scattering length.

The low-energy expansion of $a(E)$ up to the effective-range term (right-hand side of Eq. (5)) can already reproduce the realistic two-body energy for $a \gtrsim 2.5r_e$ - see Fig. 4. However at this order of expansion there are actually two solutions to Eq. (14), the lowest-energy solution being unphysical. The two solutions merge and disappear at $a = 2r_e$. The presence of this extra dimer is an artefact which completely changes the 3-body physics. Note that this problem does not occur for negative effective ranges, as in the case of narrow Feshbach resonances [41]. To remedy this problem, we consider an improved analytical expression for $a(E)$ that is obtained from the separable potential Eq. (7) adjusted to reproduce the scattering length and effective range of the scaled LM2M2 potential. Then there is only one solution to Eq. (14) and its energy matches very well that of the LM2M2 potential - see Fig. 4. Interestingly, the agreement is even slightly better than the effective-range approximation itself.

Having set $a(E)$ to properly describe two-body physics, we perform trimer calculations using Eq. (4) with a fixed cutoff P whose value is adjusted to reproduce the second 3-body dissociation point - the point where the first excited trimer reaches the threshold. One can see in Fig. 6 that the corrections bring some improvement, but the agreement with the LM2M2 results is only partial. We then determined the required variation of the cutoff P in order to obtain perfect agreement with the LM2M2 results for both the ground and first excited trimer states. The variation

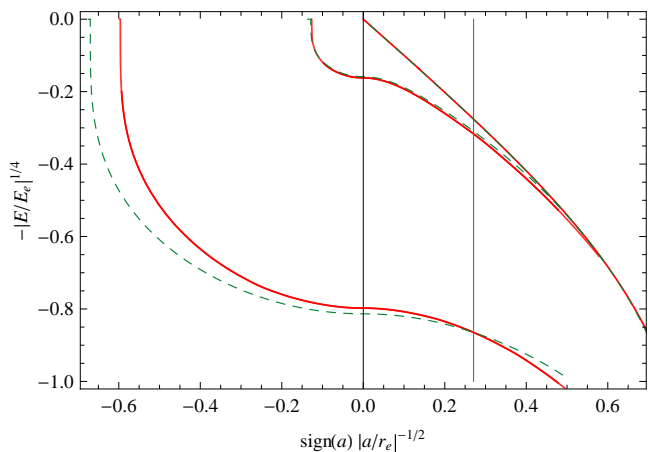


Figure 6: Similar plot to Fig. 5. Here again, the helium 4 curves are indicated by solid red curves, and results taking into account two-body corrections to the universal theory are indicated by dashed curves.

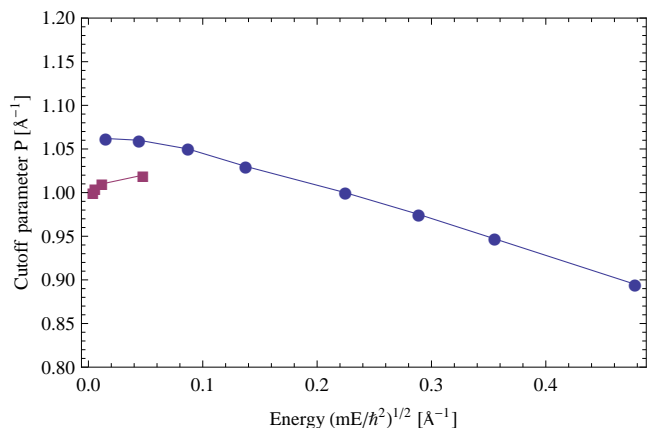


Figure 7: Three-body cutoff parameter P adjusted to get agreement with the LM2M2 results, as a function of energy, for the ground-state trimer (dots) and the excited-state trimer (squares). One can see that their variations are inconsistent.

is represented in Fig. 7 and is inconsistent for both states. To remove the inconsistency, we can assume more generally that P depends on both the energy and the scattering length, but no clear pattern arises from such considerations. It should also be noted that the required variation of P is dependent on the choice of the high-energy behaviour of $a(E)$, in other words it is model-dependent. Thus, while it can be a practical way to characterize non-universal observations, as done in Refs. [15, 16, 22], it does not seem to be very meaningful.

C. Calculations with a separable potential

We then attempt to reproduce the ^4He results with a simple two-body potential V having the same low-energy properties as the LM2M2 potential. For both the Gaussian potential (6) and separable potential (7), we proceed as follows.

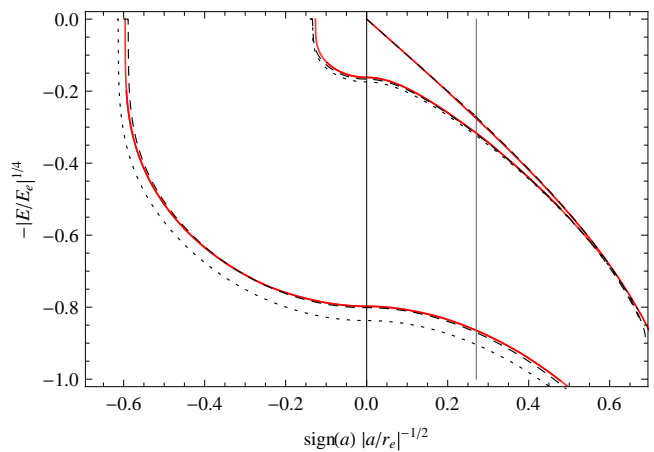


Figure 8: Similar plot to Fig. 5 for the calculations with the gaussian potential Eq. (6). The dotted curves correspond to two-body interactions only, while the dashed curves correspond to calculation with an additional three-body interaction.

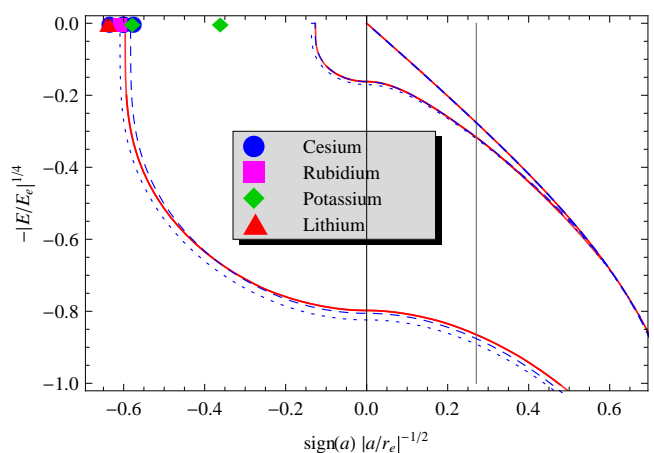


Figure 9: Similar plot to Fig. 5 for the calculations with the separable gaussian potential Eq. (7). The dotted curves correspond to two-body interactions only, while the dashed curves correspond to calculation with an additional three-body interaction. The symbols show the measured dissociation point of the ground-state trimer for different species.

For each λ , we adjust the parameters of the potential so that the scattering length and effective range coincide with those of the scaled LM2M2 potential. As mentioned before, the binding energy of the two-body bound state then matches very well that of the LM2M2 bound state over a wide range of energies - see Fig. 4.

We then calculate the three-body bound states with the adjusted potential. Remarkably, we already find relatively good agreement with the LM2M2 three-body states - see Figs. 8 and 9. The values differ essentially by an energy shift, which is not unexpected since the short-range three-body phase may not be properly set by these simple two-body interactions.

We finally add a three-body interaction (also chosen to be Gaussian or separable), and adjust its strength in order to reproduce the second three-body dissocia-

tion point. We then find very good overall agreement with the LM2M2 calculations, as shown in Figs. 8 and 9.

D. Role of the effective range

The previous results clearly indicate that the non-universal variations of the trimer energies can be reproduced to a great extent from the knowledge of the effective range. The role of the effective range was pointed out before in a previous studies [18, 19, 30, 32]. In particular, Ref. [32] also looked at deviations from universality with finite-range potentials. This study considered the scattering length a_{diss} for which the trimer dissociates. The relative variation of this quantity with respect to its value a'_{diss} in the universal spectrum was found to be:

$$\frac{a_{\text{diss}} - a'_{\text{diss}}}{a'_{\text{diss}}} = C \left(\frac{r_e}{a} \right)_{\text{diss}} \quad (15)$$

with $C = 1.3 \pm 0.4$. However, we could not completely confirm this formula. While we found the value $C \approx 0.99$ with the Gaussian potential, which is consistent with the results presented in Ref. [32] for the same Gaussian potential, the present calculation with the LM2M2 potential gives $C \approx 0.58$. The value therefore seems to be somewhat dependent on the type of potential.

It is interesting to note that the value of the dissociation point a_{diss} itself, rather than its non-universal variation, was found experimentally to be in a narrow range. Experimentalists have measured the ground-state trimer dissociation point near several divergences of the scattering lengths [17], and for different species [2, 3, 6, 9, 10, 14, 17], and found that it almost always occurs around $a_{\text{diss}} \approx -9.9\bar{a}$, where $\bar{a} = 2\pi/\Gamma(1/4)^2 l_{\text{vdW}}$ is the average scattering length of van der Waals potentials [38]. Since there is an approximate relation between \bar{a} and the effective range r_e [42, 43]:

$$\frac{r_e}{a} = \frac{2}{3} \frac{\Gamma(1/4)^4 \bar{a}}{(2\pi)^2 a} \left(\left(\frac{\bar{a}}{a} \right)^2 + \left(\frac{\bar{a}}{a} - 1 \right)^2 \right), \quad (16)$$

this corresponds to $a_{\text{diss}}/r_e \approx -2.76$. Experimental measurements of a_{diss}/r_e for different species are represented in Fig. 9. It is quite remarkable that the scaled helium potential also gives a dissociation point $a_{\text{diss}}/r_e \approx -2.82$ (or equivalently $a_{\text{diss}}/\bar{a} = -10.26$) which lies in the same narrow range. Furthermore, the model potentials considered in this paper (Gaussian and separable potential), without any 3-body interaction, also give a consistent value $a_{\text{diss}}/r_e \approx -2.70$

of the dissociation point. This shows that the use of these model potentials to interpret experiments leads to a good estimate of the dissociation point, as noted before [21, 22]. Why it does so is however a puzzling question, since we know from calculations with other or deeper potentials, that the dissociation point can change significantly [23]. This suggests that, under some condition yet to be discovered, the effective range may not only determine the non-universal variations, but also the three-body parameter, thereby determining the full three-body spectrum.

IV. CONCLUSION

In this work, we have studied the Efimov physics of three helium-4 atoms, as a simple but realistic example to understand the non-universal variations of the trimer energy with respect to the scattering length. We found that non-universal two-body corrections to the universal theory alone are not sufficient to fully reproduce these variations, and a variable three-body parameter is needed. However the variations of this three-body parameter do not seem to follow any simple rule, and are model-dependent. On the other hand, *ad hoc* but simple two-body potentials such as separable Gaussian potentials adjusted to have the same scattering length and effective range reproduce remarkably well the trimer energy non-universal variations, and can constitute relatively accurate substitutes for single-channel realistic interactions provided that a small and localised three-body force is introduced to properly shift the energy. This indicates that the non-universal deviations which were observed in [15, 16] and could not be explained by these effective potential models are likely to be due to more subtle effects such as multichannel coupling, non-trivial effects of three-body forces, unless they simply result from underestimated uncertainties either in the scattering lengths or experimental data.

Provided that such subtle effects are absent, our results also suggest that in general, beyond the usual Efimov universal scenario occurring for higher excited trimers, the whole spectrum follows a more specific class of universality determined only by the scattering length, the effective range, and the strength of a three-body localised force setting the three-body parameter, i.e. the position of highly-excited trimers.

We thank F. Ferlaino, R. Grimm, P.S. Julienne, J. D’Incao, C.H. Greene and E. Braaten for helpful discussions. Some of the numerical calculations were performed on the HITACHI SR11000 at KEK.

[1] V. N. Efimov, Sov. J. Nucl. Phys. **12**, 589 (1970) ;
V. Efimov, Nucl. Phys. A, 210, 157 (1973).
[2] F. Ferlaino and R. Grimm, Physics **3**, 9 (2010).

[3] T. Kraemer, et al. Nature **440**, 315–318 (2006).
[4] T. B. Ottenstein, et al., Phys. Rev. Lett. **101**, 203202 (2008).

- [5] J. R. Williams, et al., Phys. Rev. Lett. **103**, 130404 (2009).
- [6] M. Zaccanti, et al., Nature Physics **5**, 586 - 591 (2009).
- [7] G. Barontini et al., Phys. Rev. Lett. **103**, 043201 (2009).
- [8] A. N. Wenz, et al., Phys. Rev. **A** **80**, 040702 (2009).
- [9] S. E. Pollack, D. Dries, R. G. Hulet, Science **326**, 1683 (2009).
- [10] N. Gross, Z. Shotan, S. Kokkelmans, and L. Khaykovich, Phys. Rev. Lett. **103**, 163202 (2009).
- [11] J. H. Huckans et al., Phys. Rev. Lett. **102**, 165302 (2009).
- [12] T. Lompe, et al., Phys. Rev. Lett. **105**, 103201 (2010).
- [13] T. Lompe, et al., Science **330**, 940 (2010).
- [14] N. Gross, Z. Shotan, S. Kokkelmans, and L. Khaykovich, Phys. Rev. Lett. **105**, 103203 (2010).
- [15] S. Nakajima, M. Horikoshi, T. Mukaiyama, P. Naidon, and M. Ueda, Phys. Rev. Lett. **105**, 023201 (2010).
- [16] S. Nakajima, M. Horikoshi, T. Mukaiyama, P. Naidon, and M. Ueda, Phys. Rev. Lett. **106**, 143201 (2011).
- [17] M. Berninger et al., Phys. Rev. Lett. **107**, 120401 (2011).
- [18] Lucas Platter, Chen Ji, and Daniel R. Phillips, Phys. Rev. A **79**, 022702 (2009).
- [19] C. Ji, L. Platter, and D. R. Phillips, Europhys. Lett. **92**, 13003 (2010).
- [20] M. D. Lee, T. Köhler, and P. S. Julienne, Phys. Rev. A **76**, 012720 (2007).
- [21] M. Jona-Lasinio and L. Pricoupenko, Phys. Rev. Lett. **104**, 023201 (2010).
- [22] P. Naidon and M. Ueda, Comptes Rendus Physique, **12**, iss. 1, p. 13-26 (2011) [arXiv:1008.2260 (2010)].
- [23] J. P. D’Incao, C. H. Greene, and B. D. Esry, J. Phys. B **42**, 044016 (2009).
- [24] T. Cornelius and W. Glöckle, J. Chem. Phys. **85**, 3906 (1986).
- [25] B. D. Esry, C. D. Lin, and Chris H. Greene, Phys. Rev. A **54**, 394 (1996).
- [26] E. Nielsen, D.V. Fedorov, and A.S. Jensen, J. Phys. B **31**, 4085 (1998).
- [27] T. González-Lezana et al, Phys. Rev. Lett. **82**, 1648 (1999).
- [28] Eric Braaten, H.-W. Hammer, Phys. Rev. A **67**, 042706 (2003).
- [29] G. V. Skorniakov and K. A. Ter-Martirosian, Sov. Phys. JETP **4**, 648 (1957).
- [30] V. Efimov, Phys. Rev. C **44**, 2303 (1991).
- [31] A. Kievsky, E. Garrido, C. Romero-Redondo, and P. Barletta, Few-Body Syst DOI 10.1007/s00601-011-0226-9 (2011).
- [32] M. Thøgersen, D. V. Fedorov, and A. S. Jensen, Phys. Rev. A **78**, 020501R (2008).
- [33] R.A. Aziz, M.J. Slaman, J. Chem. Phys. **94**, 8047 (1991).
- [34] C.A. Parish and C.E. Dykstra, J. Chem. Phys. **101**, 7618 (1994).
- [35] I. Røeggen and J. Almlöf, J. Chem. Phys. **102**, 7095 (1995).
- [36] W. Cencek, M. Jeziorska, O. Akin-Ojo, and K. Szalewicz, J. Phys. Chem. A, **111** (44), 11311 (2007).
- [37] E. Hiyama, Y. Kino, and M. Kamimura, Prog. Part. and Nucl. Phys. **51**, 223 (2003).
- [38] C. Chin, R. Grimm, P. Julienne, and E. Tiesinga, Rev. Mod. Phys. **82**, 1225 (2010).
- [39] D. Blume and C. H. Greene, J. Chem. Phys. **112**, 8053 (2000).
- [40] R. Lazauskas, J. Carbonell, Phys. Rev. A **73**, 062717 (2006).
- [41] D. S. Petrov, Phys. Rev. Lett. **93**, 143201 (2004).
- [42] B. Gao, Phys. Rev. A **58**, 4222 (1998).
- [43] V.V. Flambaum, G.F. Gribakin, and C. Harabati, Phys. Rev. A **59**, 1998 (1999).